NMR Observations of Interligand Interference in the Molecular Motion of Double-Stranded Dinuclear Helicates

Hirohiko Houjou,*[a][‡] Nathanaëlle Schneider,[b] Yoshinobu Nagawa,[a] Masatoshi Kanesato,[a] Romain Ruppert,[b] and Kazuhisa Hiratani[c]

Keywords: DNA / Helical structures / NMR spectroscopy / Palladium / Schiff-base ligands

Double-stranded dinuclear complexes with either twisted or parallel arrangements were obtained by reaction between Schiff-base ligands and Pd^{II} ions. Linear ligands mainly afforded twisted arrangements, while macrocyclic ligands forced the complex to adopt parallel arrangements. In these dinuclear complexes, one isomer could not be converted into the other even upon prolonged heating. The NMR spectra showed that the chemical shifts of the diastereotopic protons can be used as an indicator to distinguish between the arrangements. The NOE cross-peak characteristics of the complexes with twisted arrangements are interpreted with reference to the crystal structure of a Cu^{II} complex as an isostructural model of the Pd^{II} complex. Variable-temperature measurements revealed the rotational interference between the ligands of the counterpart strands, the first time that this has been observed for helically arranged complexes.

Introduction

The spontaneous assembly of coordination compounds is an important tool for the construction of such fascinating architectures as a nanoscale molecule with well-defined polyhedral shape, or an infinite coordination polymer with a regularly arranged cavity.[1−4] Amongst the various three-dimensional structures, the helix is an attractive one to investigate. Many studies on helically arranged complexes have so far served as the foundation of molecular design, synthetic strategy, thermodynamics, kinetics, stereochemistry, and molecular architectonics in metallo-supramolecular chemistry.[5−7] Recently, helical complexes have been studied not only as a subject in basic chemistry, but also as a useful building block for functional materials.[8−12]

There have been many attempts to prepare double- or triple-stranded helical complexes by using metal-directed self-assembly.[13−22] For the efficient construction of helical structures the design of the linker connecting the chelating units is quite important, because a ligand could afford either a homochiral complex (helicate) with twisted arrangement or a heterochiral complex (*meso*-helicate, mesocate, or side-by-side complex) with parallel arrangement depending on the linker's shape and symmetry (Figure 1).[13] Since the potential advantages of the helical structures originate in their chirality, much attention has been paid to the thermodynamics of the complexes. It is known, for example, that in some cases the helical and nonhelical forms are in equilibrium in solution, resulting in the racemization of the compound.[23−25] This kind of dynamic interconversion is an inevitable result of entropy-driven molecular aggregation.

Another possible process to construct the helical structures is enthalpy-driven molecular aggregation, which

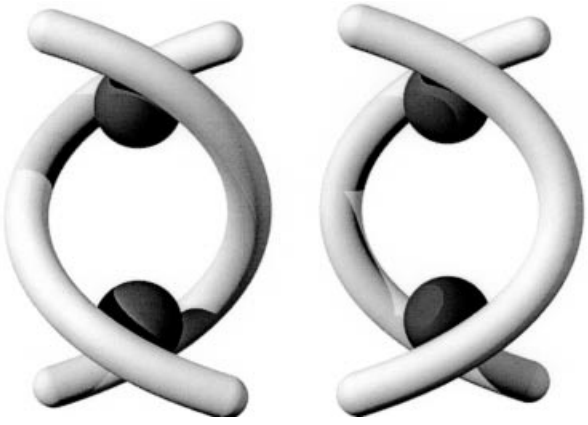

Figure 1. Model drawings of double-stranded dinuclear complexes with twisted (left) and parallel (right) arrangements

[a] Nanoarchitectonics Research Center, National Institute of Advanced Industrial Science and Technology (AIST), 1-1-1 Higashi, Tsukuba, Ibaraki 305-8562, Japan
[b] Faculté de Chimie, Université Louis Pasteur, 1 rue Blaise Pascal, 67008 Strasbourg Cedex, France
[c] Department of Applied Chemistry, Utsunomiya University, 7-2-1 Youtou, Utsunomiya 321-8585, Japan
[‡] Current address: Institute of Industrial Science, University of Tokyo, 4-6-1 Meguro-ku Tokyo 153-8505, Japan, E-mail: houjou@iis.u-tokyo.ac.jp

  DOI: 10.1002/ejic.200400407

would afford thermally stable products. However, this method has an intrinsic difficulty in controlling the products because the reaction is largely kinetically controlled. Thus, a desirable ligand should maintain a conformation suitable for the formation of a helix during the complexation. We have investigated a variety of Schiff bases containing a 2-methylenepropane-1,3-diyl (isobutenylene) chain as a linker, as a promising ligand that would fulfill this requirement.[26] We have succeeded in synthesizing dinuclear complexes of Ti^{IV}, Y^{III}, Ni^{II}, and Cu^{II}.[27–29] Among these complexes, we found that Ni^{II} and Cu^{II} species have a helical arrangement in which the coordination site adopts a square-planar geometry.[29] This finding suggested a possible access to an isostructural complex of Pd^{II}. Such complexes with diamagnetic properties could be studied by NMR techniques, leading to the understanding of their formation mechanisms as well as their structure in solution and thermodynamic behavior. In this article we describe the synthesis and characterization of Pd^{II} complexes of our Schiff-base ligands. We will highlight the difference in NMR features between the complexes with twisted and parallel arrangements. Those NMR results are successfully interpreted based on a comparative study of the crystal structures between the Pd^{II} and Cu^{II} complexes. In particular, interligand interference in molecular motion is observed for the first time for the complexes with a twisted arrangement.

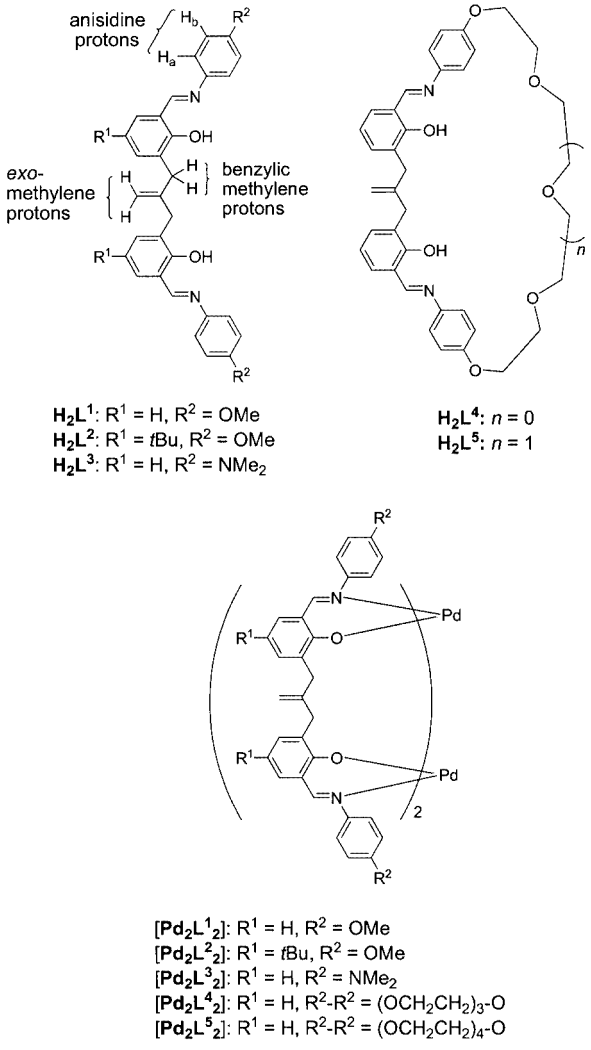

Figure 2. Chemical structures of the ligands and complexes; some specific protons referred to in the text are denoted

Results and Discussion

Characterization of the Helical and Nonhelical Complexes

The reaction of the Schiff-base ligands (H_2L^1 to H_2L^3; see Figure 2) and palladium(II) acetate afforded yellowish orange solids. The major products show ESI-MS peaks corresponding to a 2:2 assembly of ligand and palladium ion. Based on the results of our previous studies,[29] the products were expected to be the double-stranded dinuclear palladium complexes $[Pd_2L^1_2]$, $[Pd_2L^2_2]$ and $[Pd_2L^3_2]$, as shown in Figure 2. Their NMR spectra and elemental analyses were also in agreement with the proposed structure.

The ^1H NMR spectrum of $[Pd_2L^1_2]$ shows a split pair of doublets at δ = 1.87 ppm (^2J = 14.2 Hz) and 2.34 ppm (^2J = 14.2 Hz), which were assigned to the benzylic methylene protons (Figure 2) of the isobutenylene linker. This AB-type geminal coupling suggests a constraint of molecular motion which makes the two protons diastereotopic. These benzylic protons and the *exo*-methylene protons (δ = 4.75 ppm) exhibit NOE cross-peaks, among which one peak (between δ = 1.87 and 4.75 ppm) is significantly stronger than the other one (between δ = 2.34 and 4.75 ppm). These biased cross-peaks suggested a difference in distance ($d_{H\cdots H}$) between the benzylic proton and the *exo*-methylene proton. In view of the possible rotamers of the isobutenylene group,[26c,26d,30] one benzylic proton should be located in the in-plane region ($d_{H\cdots H} \approx 2.3$ Å) with respect to the π-plane of the ethylene group, while the other should be located in the out-of-plane region ($d_{H\cdots H} \approx 3.3$ Å). Therefore, we assigned the signal at δ = 1.87 ppm to the in-plane proton, and the signal at δ = 2.34 ppm to the out-of-plane proton. The NMR spectra of $[Pd_2L^2_2]$ and $[Pd_2L^3_2]$ also show similar features. The chemical shifts of the in-plane and out-of-plane protons are summarized in Table 1.

The ^1H NMR spectrum of the crude precipitate obtained after the reaction between Pd^{II} and ligand L^1 indicates the presence of a by-product that gives a split pair of doublets at δ = 2.02 and 2.20 ppm in the region of the benzylic methylene protons (Table 1). After purification, we were able to obtain a by-product-rich sample and a major product-rich sample, for which the ratio of the two components did not change even after the sample was heated at 80 °C for several hours. This indicates that these components are kinetically controlled products, which are not thermally interconvertible. The mass spectra recorded before and after the purification show no significant change, suggesting that the major product and the by-product have the same molecular weight. This observation led to the assumption that the major and minor components are two isomers with twisted and parallel arrangements (see Figure 1).

Table 1. The chemical shift[a] (in ppm) of the benzylic methylene protons, and the presumed arrangement of the complexes

Compound	In-plane proton	Out-of-plane proton	$\Delta\delta$	Arrangement
$[Pd_2L^1{}_2]$	1.87 (14.2)	2.34 (14.2)	0.47	twisted
$[Pd_2L^1{}_2]$ (by-product)	2.02 (14)	2.20 (14)	0.18	parallel
$[Pd_2L^2{}_2]$	1.88 (14.1)	2.49 (14.1)	0.61	twisted
$[Pd_2L^3{}_2]$	1.84 (14.5)	2.40 (14.4)	0.56	twisted
$[Pd_2L^4{}_2]$	2.38 (14.1)	2.53 (14.5)	0.15	parallel
$[Pd_2L^5{}_2]$	2.32 (14.5)	2.59 (14.4)	0.27	parallel

[a] Every peak appears as a doublet. The coupling constants (^2J in Hz) are given in parentheses.

To clarify the difference between the two isomers — the twisted and parallel forms — we prepared similar dinuclear palladium complexes with the ligands H_2L^4 and H_2L^5 (Figure 2) that would not allow the helical arrangement owing to their macrocyclic structure. Figure 3 shows the crystal structure of $[Pd_2L^5{}_2]$. As expected, the ligand adopts a parallel arrangement around the two palladium atoms, to which two nitrogen atoms and two oxygen atoms are bound in a slightly distorted square-planar geometry with *trans* coordination. If only electronic factors are taken into account, the coordination geometry around the palladium(II) ion is expected to be *cis* for N−O chelating ligands.[31−33] In the present case, however, since the nitrogen atom is substituted by an aromatic group, the geometry around the palladium ion is defined by steric factors. Although the crystallographic symmetry of $[Pd_2L^5{}_2]$ is C_i, the NMR spectra show a C_{2h}-like behavior of the molecule, probably due to thermal fluctuations.

The ^{1}H NMR spectra of $[Pd_2L^4{}_2]$ and $[Pd_2L^5{}_2]$ show a split pair of doublets, which are again assigned to the benzylic protons (Table 1). The pattern of these signals is similar to that observed for $[Pd_2L^1{}_2]$ to $[Pd_2L^3{}_2]$, except that the resonances are significantly shifted downfield. Table 1 also lists the difference ($\Delta\delta$) of chemical shift between the out-of-plane and in-plane protons. It should be noticed that the $\Delta\delta$ values (0.15 and 0.27 ppm) measured for complexes $[Pd_2L^4{}_2]$ and $[Pd_2L^5{}_2]$, respectively, are much lower than those found for complexes $[Pd_2L^1{}_2]$ to $[Pd_2L^3{}_2]$ (0.47−0.61 ppm), and are very close to the $\Delta\delta$ value (0.18 ppm) measured for the by-product formed along with $[Pd_2L^1{}_2]$. These distinctive $\Delta\delta$ values may arise from differences in the chemical environment of the benzylic methylene groups in the twisted arrangement and in the parallel one. In other words, the $\Delta\delta$ value can be an indicator of the arrangement of the complexes. Based on the above results, we presume that $[Pd_2L^1{}_2]$ to $[Pd_2L^3{}_2]$ have a twisted arrangement, while $[Pd_2L^4{}_2]$, $[Pd_2L^5{}_2]$, and the by-product of $[Pd_2L^1{}_2]$ have a parallel arrangement (Table 1).

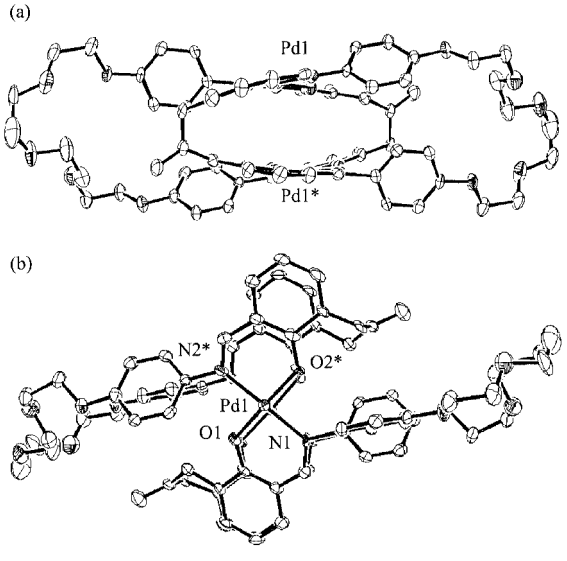

Figure 3. Crystal structure of $[Pd_2L^5{}_2]$: (a) view from the direction perpendicular to the Pd1···Pd1* line (pseudo-C_2 axis); (b) view nearly along the pseudo-C_2 axis; selected interatomic distances [Å] and bond angles [°]: O1−Pd1 1.995, O2*−Pd1 1.977, N1−Pd1 2.024, N2*−Pd1 2.042, Pd1−Pd1* 4.151; O1−Pd1−O2* 172.0, N1−Pd1−N2* 172.2; the hydrogen atoms have been omitted for clarity

NMR Features in Helical Complexes

An analysis of the crystal structures would provide helpful information to interpret the NMR spectra. Although the crystal structures of $[Pd_2L^1{}_2]$ to $[Pd_2L^4{}_2]$ have not been obtained, a comparison of the crystal structures between palladium and copper complexes confirms the assumption that these complexes have very similar structures. As shown in Figure 4, the crystal structure of $[Cu_2L^5{}_2]$ is highly reminiscent of that described above for $[Pd_2L^5{}_2]$ (see Figure 3). As expected, as copper is a first-row transition metal and palladium a second-row one, the main differences are found in the M−O and M−N distances; the other main interatomic distances in the two complexes are very close. For example, the distance between the two *exo*-methylene carbon atoms of $[Pd_2L^5{}_2]$ is 12.768 Å, while that of $[Cu_2L^5{}_2]$ is 12.685 Å, a difference of only 0.7%. Figure 5 shows the crystal structure of $[Cu_2L^2{}_2]$, which demonstrates the helical arrangement of the ligands around the two copper atoms.[12] In spite of the difference in arrangement, the geometry around each coordination site of $[Cu_2L^2{}_2]$ is quite similar to that of $[Cu_2L^5{}_2]$. From all these observations, it is reasonable to assume that the structure of $[Pd_2L^2{}_2]$ is also similar to that of $[Cu_2L^2{}_2]$.

The NOESY spectra of $[Pd_2L^1{}_2]$ to $[Pd_2L^3{}_2]$ show the characteristic cross-peaks that would be expected from a twisted arrangement. For $[Pd_2L^2{}_2]$, for example, we observed correlation peaks between the *tert*-butyl protons and the methoxy protons of the anisidine unit, and between the benzylic protons out of the plane of the ethylene group and

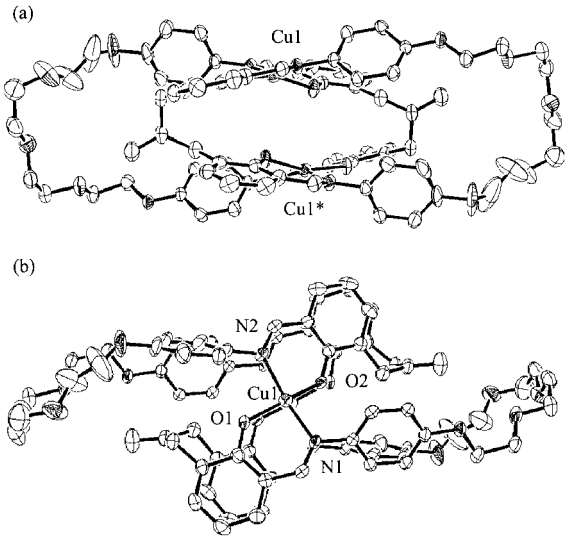

Figure 4. Crystal structure of $[Cu_2L^5_2]$: (a) view from the direction perpendicular to the Cu1···Cu1* line (pseudo-C_2 axis); (b) view nearly along the pseudo-C_2 axis; selected interatomic distances [Å] and bond angles [°]: O1−Cu1 1.881, O2−Cu1 1.892, N1−Cu1 2.002, N2−Cu1 1.999, Cu1−Cu1* 4.113; O1−Cu1−O2* 161.0, N1−Cu1−N2 158.6; the hydrogen atoms and the solvent of crystallization ($CHCl_3$) have been omitted for clarity

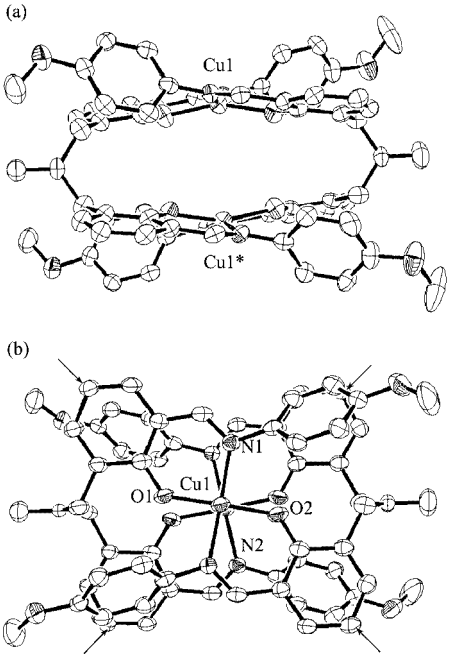

Figure 5. Crystal structure of $[Cu_2L^2_2]$: (a) view from the direction perpendicular to the Cu1···Cu1* line (pseudo-C_2 axis); (b) view nearly along the pseudo-C_2 axis; selected interatomic distances [Å] and bond angles [°]: O1−Cu1 1.880, O2−Cu1 1.864, N1−Cu1 1.984, N2−Cu1 1.991, Cu1−Cu1* 3.887; O1−Cu1−O2 159.2, N1−Cu1−N2 161.2; the hydrogen atoms and the solvent of crystallization (CH_2Cl_2) have been omitted for clarity; the *tert*-butyl groups have also been omitted for clarity, but the four carbon atoms to which they are attached are indicated by arrows in (b)

the aromatic protons (H_a and H_b, see Figure 2) of the anisidine unit. For a better understanding of these NOESY results, we analyzed the crystal structure of $[Cu_2L^2_2]$ as a model of $[Pd_2L^2_2]$. Figure 6 shows a partial structure of $[Cu_2L^2_2]$ in which the hydrogen atoms of interest are noted. The distances between the protons accurately account for the cross-peaks. First, the protons of the *tert*-butyl groups of the ligand are close to the methoxy group protons of the anisidine units of its counterpart (dashed lines A in Figure 6). This type of contact occurs only when the complex adopts a twisted arrangement. Secondly, the out-of-plane protons of the ligand are in close proximity to the anisidine units of its counterpart (dashed lines B and C in Figure 6). In addition, Figure 6 clearly shows the arrangement of the in-plane and out-of-plane benzylic protons (dashed lines D in Figure 6), which could cause the biased NOE cross-peak signals with the *exo*-methylene proton. Similarly, we were able to explain the NOE cross-peaks of the complexes with parallel arrangements — $[Pd_2L^4_2]$ and $[Pd_2L^5_2]$ — on the basis of the crystal structure of $[Pd_2L^5_2]$ (Figure 3).

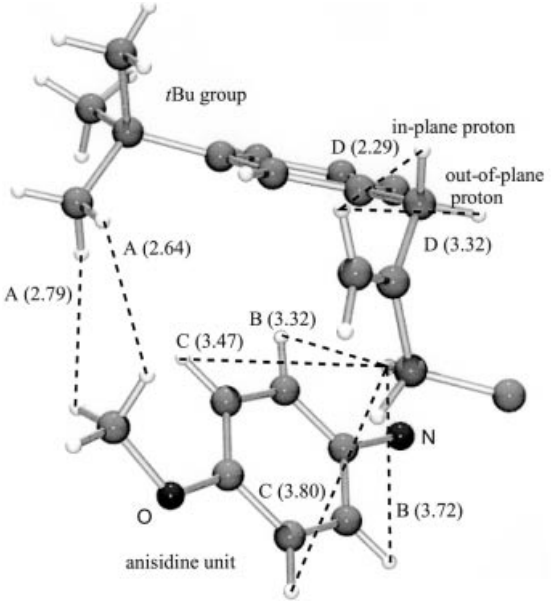

Figure 6. The crystal structure of $[Cu_2L^2_2]$ as a model of $[Pd_2L^2_2]$; notations A−D indicate a pair of protons in close proximity and their distance (in parentheses [Å])

Variable-temperature NMR measurements revealed a critical difference between the complexes with twisted and parallel arrangements. For $[Pd_2L^2_2]$, the H_a and H_b signals (anisidine protons denoted in Figure 2) appear as two doublets at $\delta = 6.56$ and 6.29 ppm, respectively, at 323 K, indicating that the anisidine ring freely rotates within the NMR timescale. At 213 K, as indicated by dashed lines in Figure 7, the H_a signal splits into two doublets at $\delta = 7.13$ and $\delta = 6.02$ ppm, while the H_b signal splits into two doublets at $\delta = 6.67$ and 5.81 ppm. The coalescence temperature is close to 253 K for both H_a and H_b. This spectral change suggests that the four protons become chemically inequivalent due to interference in the rotation of the anisidine moieties. Based on the temperature dependence of the line

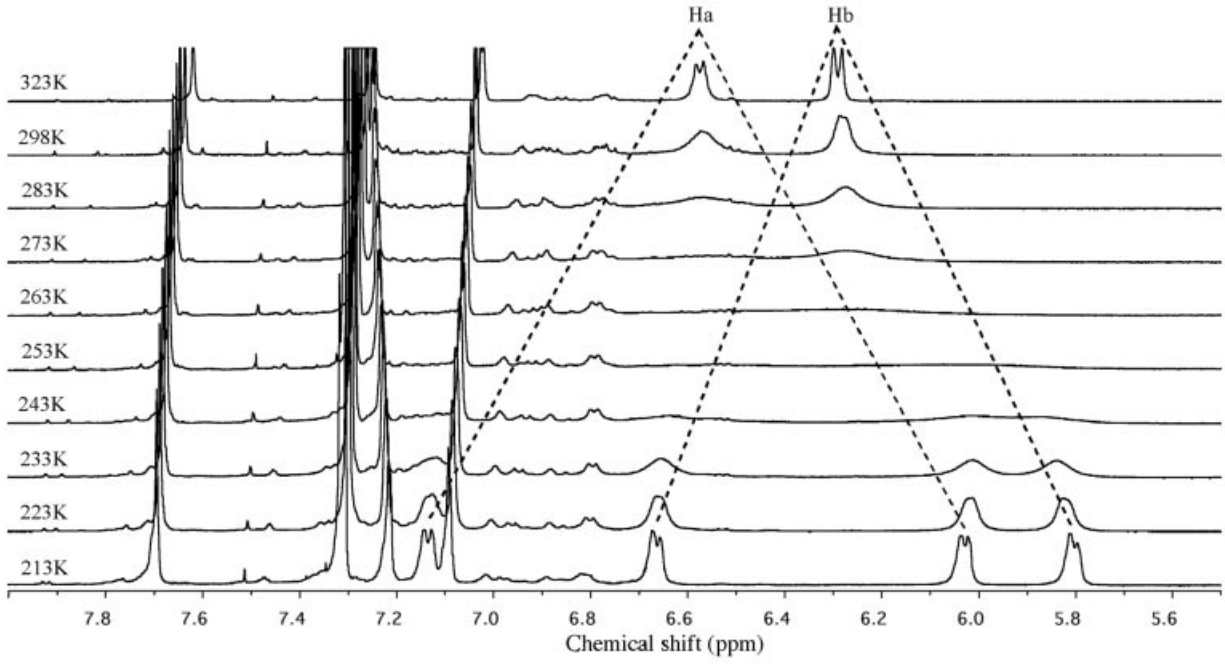

Figure 7. The temperature dependence of the ^{1}H NMR signals of the anisidine protons H_a and H_b

shape, the rotational barrier was estimated to be 47.8 kJ/mol. A similar temperature dependence was observed for $[Pd_2L^1_2]$, but with a lower coalescence temperature (243 K) and lower rotational barrier (45.4 kJ/mol). The difference in the barrier is attributable to the *tert*-butyl group on the phenolate, implying that the phenolate moiety acts as a hindrance to the rotating anisidine moiety. An influence due to contact with the benzylic methylene group is ruled out because a similar contact is also observed in the parallel complexes, which do not show interference in the anisidine rotation. To explain these phenomena, we need to assume a close contact between the anisidine moiety of one ligand and the phenolate moiety of the other, as shown in Figure 6, since the approach of these two moieties would be impossible in a single ligand molecule. Consequently, such an interligand steric hindrance is a phenomenon exclusively observed for the complexes with a twisted arrangement. On the other hand, the corresponding ^{1}H NMR signals of the complex with a parallel arrangement show little dependence on temperature. For example, the signals of H_a and H_b of $[Pd_2L^5_2]$ are observed as two doublets at δ = 7.20 and 6.87 ppm at 298 K, and they show only a slight shift to δ = 7.09 and 6.79 ppm, respectively, at 213 K.

Remarks on the Formation Mechanism

As described above, several characteristic NMR features enable us to distinguish the arrangement of the dinuclear Pd^{II} complexes. With the ligand H_2L^1, we obtained two isomers, namely the twisted form as a major product and the parallel form as a by-product. These isomers could not be interconverted, even after prolonged heating, demonstrating their thermodynamic stability. Similarly, for the other two linear ligands (H_2L^2 and H_2L^3), the major product of the reaction is the twisted isomer. By contrast, when the ligands have mechanical constraints due to their macrocyclic structures (H_2L^4 and H_2L^5), the parallel forms are the major reaction products. These results suggest that the acyclic ligands prefer a conformation that can induce a twisted arrangement in the dinuclear complexes. At this point it is worth mentioning the nature of the linker unit connecting the two chelating units in terms of symmetry. Albrecht et al. have introduced the "even-odd principle", which accounts for the relation between the arrangement and the ligand used to actively control the formation of helicates and *meso*-helicates.[34] Namely, an alkyl chain with an even number of methylene units has C_2 symmetry, which favors a helicate, whereas an alkyl chain with an odd number of methylene units has C_{2v} symmetry, which favors a *meso*-helicate. As for the present system, the isobutenylene chain can adopt several stable conformers with various symmetry such as skew-skew (C_2 symmetry), *syn-syn* (C_{2v} symmetry) and skew-skew′ (C_s symmetry). As already remarked in the previous paper, the isobutenylene chains have the skew-skew form in the helical Ni^{II} and Cu^{II} complexes. Since the helical Pd^{II} complexes are suggested to be isostructural to them, the chains should also adopt the skew-skew form. As for the nonhelical complexes, Figure 3 shows that the isobutenylene chains of $[Pd_2L^5_2]$ adopt the skew-skew′ form. According to an ab initio study (MP2/6-311**G//HF/6-311G** level of theory) of model compounds, the skew-skew form is more stable than the skew-skew′ form by 8.28 kJ/mol.[30] Although the calculated energy difference is rather small, it is suggested that the thermodynamic preference for the skew-skew conformation contributes to the efficient formation of the helical complexes to some extent.

Consequently, the present system is a good example of enthalpy-driven molecular aggregation during which the ligand component effectively controls the arrangement of the products.

Conclusion

We have described the synthesis and structure of several dinuclear palladium(II) complexes of double-stranded Schiff-base ligands with either twisted or parallel arrangements. In the present system the complexation is enthalpy driven, and the product is largely kinetically controlled. Due to this formation mechanism, the twisted and parallel isomers are thermodynamically inconvertible in solution, such that we can observe the characteristic NMR features of a given complex with a definite arrangement. To the best of our knowledge, this is the first work that clearly exhibits the interligand interactions exclusively brought into helically arranged complexes.

Experimental Section

Measurements: NMR measurements were performed using a Bruker AVANCE500 (500 MHz for ^{1}H nuclei) spectrometer. The temperature was set at 298 K unless otherwise noted. The samples were dissolved in $CDCl_3$, and TMS was used as an internal standard. The chemical shifts of ^{1}H and ^{13}C nuclei were assigned by using NOESY, ROESY, COSY, and DQF-COSY techniques. Variable-temperature measurements were performed for dynamic NMR spectroscopic analysis. Calculations for complete line-shape analyses were carried out with an IBM R-32 computer using the computer program g NMR version 4.1.[35] Theoretical spectra were calculated to obtain an optimum fit with the observed spectra by varying the exchange-rate constants. The activation parameters were obtained using the Eyring equation.[36]

For X-ray diffraction of a single crystal, the data were collected with a Rigaku RAXIS-RAPID Imaging Plate diffractometer, λ(Mo-K_α) = 0.7107 Å radiation. The structure was solved by direct methods and expanded using Fourier techniques. The nonhydrogen atoms' coordinates were refined anisotropically. Hydrogen atoms' coordinates were calculated. The final cycle of full-matrix least-squares refinement was based on the observed reflections with $I > 1.5\sigma(I)$ and variable parameters. The refinement converged with the unweighted and weighted agreement factors, R_1 and R_w. All the calculations were performed with RIGAKU Corporation's Crystal-Structure software package.[37] ORTEP drawings were created with ellipsoids of 50% probability by using the ORTEP-3 software package.[38]

Synthesis of the Pd^{II} Complexes: The Schiff-base ligands H_2L^1 to H_2L^5 (Figure 2) were prepared from the corresponding bis(hydroxybenzaldehyde) and aniline derivative according to reported methods.[26] For example, a stoichiometric amount (L^1/Pd = 1:1) of palladium(II) acetate and a few drops of methanol and acetonitrile were added to a solution of H_2L^1 (507 mg, 1.0 mmol) in chloroform (10 mL). The solution was stirred at 25 °C for several days. After confirming the disappearance of the starting material by TLC, a large quantity of methanol was added to precipitate a yellowish orange solid. Similarly, ligands H_2L^2 to H_2L^5 were allowed to react with the palladium salt. Since we found it difficult to elute the products from a silica gel column, we attempted the purification by reprecipitation from a diethyl ether/chloroform system.

[Pd$_2$L$^1_2$]: Yield: 61 mg (10%). ^{1}H NMR: δ = 1.87 (d, J = 14.2 Hz, 4 H, Ar−CH_2−), 2.34 (d, J = 14.2 Hz, 4 H, Ar−CH_2−), 3.64 (s, 12 H, −OCH_3), 4.73 [s, 4 H, −C(=CH_2)−], 6.31 (d, J = 8.0 Hz, 8 H, ArH−OCH$_3$), 6.60 (dd, J = 7.4 Hz, 7.3 Hz, 4 H, ArH−OPd), 6.61 (d, J = 7.4 Hz, 8 H, ArH−OCH$_3$), 7.09 (d, J = 7.3 Hz, 4 H, ArH−OPd), 7.11 (d, J = 7.6 Hz, 4 H, ArH−OPd), 7.61 (s, 4 H, −CH=N−) ppm. ^{13}C NMR (213 K): δ = 32.8, 55.7, 111.6, 113.1, 114.0, 114.4, 118.7, 124.7, 125.0, 131.8, 132.8, 134.3, 142.7, 149.9, 156.9, 162.6, 162.9 ppm. ESI(+) MS: m/z = 1245.5 (calcd. for [M + Na$^+$] 1245.0). IR (KBr): $\nu_{C=N}$ = 1609 cm^{-1}. $C_{64}H_{56}N_4O_8Pd_2$ (1221.97): calcd. C 62.90, H 4.62, N 4.58; found C 63.03, H 4.71, N 4.51.

[Pd$_2$L$^2_2$]: Yield: 72 mg (10%). ^{1}H NMR: δ = 1.30 [s, 36 H, −C(CH_3)$_3$], 1.88 (d, J = 14.1 Hz, 4 H, Ar−CH_2−), 2.49 (d, J = 14.1 Hz, 4 H, Ar−CH_2−), 3.61 (s, 12 H, −OCH_3), 4.78 [s, 4 H, −C(=CH_2)−], 6.29 (m, 8 H, ArH−OCH$_3$), 6.57 (m, 8 H, ArH−OCH$_3$), 7.03 (d, J = 2.7 Hz, 4 H, ArH−OPd), 7.25 (d, J = 2.0 Hz, 4 H, ArH−OPd), 7.64 (s, 4 H, −CH=N−) ppm. ^{13}C NMR (213 K): δ = 31.5, 32.9, 33.6, 55.6, 111.3, 112.6, 114.4, 117.7, 125.0, 125.2, 128.0, 130.9, 132.2, 135.8, 143.3, 151.0, 156.6, 161.3, 163.1 ppm. ESI(+) MS: m/z = 1469.6 (calcd. for [M + Na$^+$] 1269.4). IR (KBr): $\nu_{C=N}$ = 1613 cm^{-1}. $C_{80}H_{88}N_4O_8Pd_2(H_2O)_3$ (1500.43): calcd. C 64.03, H 6.31, N 3.73; found C 64.17, H 6.23, N 3.64.

[Pd$_2$L$^3_2$]: Yield: 427 mg (67%). ^{1}H NMR: δ = 1.84 (d, J = 14.5 Hz, 4 H, Ar−CH_2−), 2.40 (d, J = 14.4 Hz, 4 H, Ar−CH_2−), 2.78 [s, 24 H, −N(CH_3)$_2$], 4.68 [s, 4 H, −C(=CH_2)−], 6.16 [d, J = 8.0 Hz, 8 H, ArH−N(CH$_3$)$_2$], 6.56 (dd, J = 7.5 Hz, 7.5 Hz, 4 H, ArH−OPd), 6.57 [d, J = 7.6 Hz, 8 H, ArH−N(CH$_3$)$_2$], 7.05 (d, J = 6.6 Hz, 4 H, ArH−OPd), 7.07 (d, J = 7.9 Hz, 4 H, ArH−OPd), 7.62 (s, 4 H, −CH=N−) ppm. ^{13}C NMR (298 K): δ = 33.2, 41.2, 112.2, 112.8, 114.1, 119.3, 124.8, 132.1, 132.5, 133.9, 140.8, 149.1, 151.3, 162.5, 163.7 ppm. ESI(+) MS: m/z = 1297.2 (calcd. for [M + Na$^+$] 1297.1). IR (KBr): $\nu_{C=N}$ = 1611 cm^{-1}. $C_{68}H_{68}N_8O_4Pd_2(H_2O)_{0.5}$ (1283.15): calcd. C 63.65, H 5.42, N 8.73; found C 63.72, H 5.30, N 8.49.

[Pd$_2$L$^4_2$]: Yield: 293 mg (42%). ^{1}H NMR: δ = 2.38 (d, J = 14.1 Hz, 4 H, Ar−CH_2−), 2.53 (d, J = 14.5 Hz, 4 H, Ar−CH_2−), 3.79 (s, 8 H, −OCH_2CH_2O−), 3.89 (m, 8 H, Ar−OCH$_2$CH_2O−), 4.26 (m, 8 H, Ar−OCH_2CH$_2$O−), 4.76 [s, 4 H, −C(=CH_2)−], 6.02 (dd, J = 7.3 Hz, 7.5 Hz, 4 H, ArH−OPd), 6.58 (d, J = 7.5 Hz, 4 H, ArH−OPd), 6.64 (d, J = 8.0 Hz, 4 H, ArH−OPd), 6.93 (d, J = 8.6 Hz, 8 H, ArH−OCH$_2$−), 7.14 (d, J = 8.6 Hz, 4 H, ArH−OCH$_2$−), 7.46 (s, 4 H, −CH=N−) ppm. The ^{13}C NMR spectrum was not measured due to low solubility. ESI(+) MS: m/z = 1417.2 (calcd. for [M + Na$^+$] 1417.1). IR (KBr): $\nu_{C=N}$ = 1610 cm^{-1}. $C_{72}H_{68}N_4O_{12}Pd_2$ (1394.14): calcd. C 62.03, H 4.92, N 4.02; found C 61.81, H 5.07, N 4.13.

[Pd$_2$L$^5_2$]: Yield: 348 mg (47%). ^{1}H NMR: δ = 2.32 (d, J = 14.5 Hz, 4 H, Ar−CH_2−), 2.59 (d, J = 14.4 Hz, 4 H, Ar−CH_2−), 3.81 (m, 16 H, −OCH_2CH_2O−), 3.93 (m, 8 H, Ar−OCH$_2$CH_2O−), 4.18 (m, 8 H, Ar−OCH_2CH$_2$O−), 4.75 [s, 4 H, −C(=CH_2)−], 6.02 (dd, J = 7.3 Hz, 7.3 Hz, 4 H, ArH−OPd), 6.59 (d, J = 6.7 Hz, 4 H, ArH−OPd), 6.61 (d, J = 7.8 Hz, 4 H, ArH−OPd), 6.87 (d, J = 8.7 Hz, 8 H, ArH−OCH$_2$−), 7.20 (d, J = 8.7 Hz, 4 H, ArH−OCH$_2$−), 7.47 (s, 4 H, −CH=N−) ppm. ^{13}C NMR (213 K): δ = 35.0, 66.5, 67.9, 69.7, 69.2, 112.7, 112.7, 113.0, 116.7, 125.2, 129.2, 130.7, 132.7, 142.2, 147.5, 155.5, 160.9, 161.6 ppm. ESI(+) MS: m/z = 1505.4 (calcd. for [M + Na$^+$] 1505.2). IR (KBr):

$\nu_{C=N}$ = 1609 cm^{-1}. $C_{76}H_{76}N_4O_{14}Pd_2(H_2O)_3$ (1536.30): calcd. C 59.41, H 5.38, N 3.65; found C 58.99, H 4.98, N 3.40. A single crystal suitable for X-ray analysis was obtained by recrystallization from chloroform/diethyl ether. Crystal data: $C_{38}H_{38}N_2O_7Pd$ (741.12); crystal system: monoclinic; space group: *C*2/*c* (no. 15); Z = 8 in a cell of dimensions a = 21.259(8), b = 19.594(6), c = 17.239(6) Å, β = 111.15(3)°, V = 6697.2(4) $Å^3$, $D_{calcd.}$ = 1.470 g/cm^3, μ = 6.11 cm^{-1}, 30806 measured and 7612 unique reflections ($2\theta_{max}$ = 55.0°, R_{int} = 0.128); R_1 = 0.045, R_w = 0.082.

Synthesis of $[Cu_2L^5_2]$: A methanol solution (25 mL) of copper(II) acetate monohydrate (20 mg, 0.1 mmol) was added to a solution of H_2L^5 (64 mg, 0.1 mmol) in chloroform (25 mL). The solution was left at 25 °C without stirring for several hours. The resultant precipitate was collected by filtration. Yield: 64 mg (92%). ESI(+) MS: *m*/*z* = 1419.3 (calcd. for [M + Na^+] 1419.5). IR (KBr): $\nu_{C=N}$ = 1611 cm^{-1}. $C_{76}H_{76}Cu_2N_4O_{14}(CHCl_3)_2$ (1635.25): calcd. C 57.36, H 4.81, N 3.43; found C 57.97, H 4.38, N 3.31. A single crystal as precipitated was used for the X-ray analysis. Crystal data: $C_{38}H_{38}CuN_2O_7(CHCl_3)_2$ (937.03); crystal system: triclinic; space group: $P\bar{1}$ (no. 2); Z = 2 in a cell of dimensions a = 11.968(1), b = 12.0109(9), c = 17.706(2) Å, α = 74.666(5)°, β = 70.671(4)°, γ = 60.561(4)°, V = 2075.6(3) $Å^3$, $D_{calcd.}$ = 1.499 g/cm^3; μ = 9.63 cm^{-1}, 19156 measured and 8909 unique reflections ($2\theta_{max}$ = 54.8°, R_{int} = 0.040); R_1 = 0.084, R_w = 0.211.

Acknowledgments

Predoctoral fellowships for N. S. by the Région Alsace and the Chemistry Department of the Université Louis Pasteur are acknowledged.

[1] M. Fujita, K. Umemoto, M. Yoshizawa, N. Fujita, T. Kusukawa, K. Biradha, *Chem. Commun.* **2001**, 509−518.
[2] B. J. Holliday, C. A. Mirkin, *Angew. Chem. Int. Ed.* **2001**, *40*, 2022−2043.
[3] O. M. Yaghi, M. O'Keeffe, N. W. Ocking, H. K. Chae, M. Eddaoudi, J. Kim, *Nature* **2003**, *423*, 705−714.
[4] S. Kitagawa, M. Kondo, *Bull. Chem. Soc. Jpn.* **1998**, *71*, 1739−1753.
[5] J.-M. Lehn, *Supramolecular Chemistry: Concepts and Perspectives*, VCH, Weinheim, **1995**.
[6] E. C. Constable, *Metals and Ligand Reactivity*, VCH, Weinheim, **1996**.
[7] *Transition Metals in Supramolecular Chemistry* (Ed.: J.-P. Sauvage), John Wiley & Sons, Chichester, **1999**.
[8] R. Ziessel, *Coord. Chem. Rev.* **2001**, *216−217*, 195−223.
[9] L. Brunsveld, E. W. Meijer, R. B. Prince, J. S. Moore, *J. Am. Chem. Soc.* **2001**, *123*, 7978−7984.
[10] H.-C. Zhang, W.-S. Huang, L. Pu, *J. Org. Chem.* **2001**, *66*, 481−487.
[11] A. Lavalette, J. Hamblin, A. Marsh, D. M. Haddleton, M. J. Hannon, *Chem. Commun.* **2002**, 3040−3041.
[12] H. Houjou, Y. Shimizu, N. Koshizaki, M. Kanesato, *Adv. Mater.* **2003**, *15*, 1458−1461.
[13] M. Albrecht, *Chem. Rev.* **2001**, *101*, 3457−3479.
[14] E. C. Constable, M. J. Hannon, D. A. Tocher, *Angew. Chem. Int. Ed. Engl.* **1992**, *31*, 230−232.
[15] S. Ruettimann, C. Piguet, G. Brenardinelli, B. Bocquet, A. F. Williams, *J. Am. Chem. Soc.* **1992**, *114*, 4230−4237.
[16] D. E. Fenton, R. W. Matthews, M. McPartlin, B. P. Murphy, I. J. Scowen, P. A. Tasker, *J. Chem. Soc., Chem. Commun.* **1994**, 1391−1392.
[17] [17a] J. Hamblin, A. Jackson, N. W. Alcock, M. J. Hannon, *J. Chem. Soc., Dalton Trans.* **2002**, 1635−1641. [17b] J. Hamblin, L. J. Childs, N. W. Alcock, M. J. Hannon, *J. Chem. Soc., Dalton Trans.* **2002**, 164−169. [17c] M. J. Hannon, S. Bunce, A. J. Clarke, N. W. Alcock, *Angew. Chem. Int. Ed.* **1999**, *38*, 1277−1278.
[18] [18a] M. Elhabiri, R. Scopelliti, J.-C. G. Bünzli, C. Piguet, *J. Am. Chem. Soc.* **1999**, *121*, 10747−10762. [18b] J.-C. G. Bünzli, C. Piguet, *Chem. Rev.* **2002**, *102*, 1897−1928.
[19] [19a] C. O. Dietrich-Buchecker, J.-P. Sauvage, A. De Cian, J. Fischer, *J. Chem. Soc., Chem. Commun.* **1994**, 2231−2232. [19b] G. Rapenne, B. T. Patterson, J. -P. Sauvage, F. R. Keene, *Chem. Commun.* **1999**, 1853−1854.
[20] B. Hasenknopf, J.-M. Lehn, N. Boumediene, A. Dupont−Gervais, A. Van Dorsselaer, B. Kneisel, D. Fenske, *J. Am. Chem. Soc.* **1997**, *119*, 10956.
[21] [21a] P. L. Jones, K. J. Byrom, J. C. Jeffery, J. A. McCleverty, M. D. Ward, *Chem. Commun.* **1997**, 1361−1362. [21b] M. D. Ward, J. A. McCleverty, J. C. Jeffery, *Coord. Chem. Rev.* **2002**, *222*, 251−272.
[22] [22a] M. Albrecht, R. Fröhlich, *J. Am. Chem. Soc.* **1997**, *119*, 1656−1661. [22b] M. Albrecht, *Chem. Soc. Rev.* **1998**, *27*, 281−287. [22c] M. Albrecht, O. Blau, R. Fröhlich, *Proc. Natl. Acad. Sci. USA* **2002**, *99*, 4867−4872.
[23] [23a] P. Comba, A. Fath, T. W. Hambley, A. Vielfort, *J. Chem. Soc., Dalton Trans.* **1997**, 1691−1695. [23b] P. Comba, A. Kuener and A Peters, *J. Chem. Soc., Dalton Trans.* **1999**, 509−516.
[24] J. Xu, T. N. Parac, K. Raymond, *Angew. Chem. Int. Ed.* **1999**, *38*, 2878−2882.
[25] M. Elhabiri, J. Hamacek, J.-C. G. Bünzli, A.-M. Albrecht-Gary, *Eur. J. Inorg. Chem.* **2004**, 51−62.
[26] [26a] H. Houjou, S.-K. Lee, Y. Hishikawa, Y. Nagawa, K. Hiratani, *Chem. Commun.* **2000**, 2197−2198. [26b] H. Houjou, Y. Nagawa, K. Hiratani, *Tetrahedron Lett.* **2001**, *42*, 3861−3863. [26c] H. Houjou, S. Tsuzuki, Y. Nagawa, K. Hiratani, *Bull. Chem. Soc. Jpn.* **2002**, *75*, 831−839. [26d] H. Houjou, S. Tsuzuki, Y. Nagawa, M. Kanesato, K. Hiratani, *Bull. Chem. Soc. Jpn.* **2003**, *76*, 2405−2411.
[27] M. L. N. Rao, H. Houjou, K. Hiratani, *Chem. Commun.* **2002**, 420−421.
[28] M. Kanesato, H. Houjou, Y. Nagawa, K. Hiratani, *Inorg. Chem. Commun.* **2002**, *5*, 984−988.
[29] H. Houjou, A. Iwasaki, T. Ogihara, M. Kanesato, S. Akabori, K. Hiratani, *New J. Chem.* **2003**, *27*, 886−889.
[30] S. Tsuzuki, H. Houjou, Y. Nagawa, K. Hiratani, *J. Chem. Soc., Perkin Trans. 2* **2000**, 2448−2452.
[31] R. H. Holm, M. J. O'Connor, *Prog. Inorg. Chem.* **1971**, *14*, 241−401.
[32] A. W. Maverick, F. R. Fronczek, D. P. Martone, J. R. Bradbury, *J. Coord. Chem.* **1989**, *20*, 149−161.
[33] S. Richeter, C. Jeandon, J.-P. Gisselbrecht, R. Graff, R. Ruppert, H. J. Callot, *Inorg. Chem.* **2004**, *43*, 251−263.
[34] M. Albrecht, *Chem. Eur. J.* **2000**, *6*, 3485−3489.
[35] P. H. M. Budzelaar, *Simulation of One-Dimensional NMR Spectra*, Cherwell Scientific Limited, Oxford, **1999**.
[36] M. Oki, *Application of Dynamic NMR Spectroscopy to Organic Chemistry, Methods in Stereochemical Analysis*, vol. 4, VCH, Orlando, **1985**.
[37] *CrystalStructure*, version 3.10, Rigaku Coorporation and Rigaku/MSC, Tokyo, Japan, **2002**.
[38] ORTEP-3 for Windows: L. J. Farrugia, *J. Appl. Crystallogr.* **1997**, *30*, 565.

Received May 16, 2004
Early View Article
Published Online September 7, 2004

